0026-895X/94/061197-07$03.00/0

MOLECULAR PHARMACOLOGY, 46:1197–1203, 1994.

γ-Aminobutyric Acid Type A Receptor Antagonists Picrotoxin and Bicuculline Alter Acetylcholine Channel Kinetics in Cultured Embryonic Rat Skeletal Muscle

QI-YING LIU, VERONICA DUNLAP, and JEFFERY L. BARKER

Laboratory of Neurophysiology, National Institute of Neurological Disorders and Stroke, National Institutes of Health, Bethesda, Maryland 20892

Received July 20, 1994; Accepted September 13, 1994

SUMMARY

The effects of the classical γ-aminobutyric acid type A receptor antagonists picrotoxin and bicuculline on nicotinic acetylcholine receptors in cultured embryonic rat skeletal muscle were examined with whole-cell and cell-attached single-channel recording methods. Up to 600 μM picrotoxin had little or no effect on the amplitude of the whole-cell current, whereas bicuculline dose-dependently blocked it, with an IC_{50} value of 101.2 ± 8.9 μM. Bicuculline reduced the maximum inducible acetylcholine current without changing the K_d value, suggesting that bicuculline uncompetitively blocked the binding of acetylcholine to its receptor. The elementary nicotinic acetylcholine receptor currents recorded in the cell-attached single-channel recording configuration exhibited properties typical of those recorded in embryonic muscle (~36 pS and ~6 msec). Picrotoxin dramatically transformed individual channel openings into briefly interrupted bursts, so that the number of openings increased while the mean open time markedly decreased. Bicuculline decreased mean open time to a lesser but statistically significant degree. The dominant component of the closed time histogram in control recordings occurred at 17 msec, whereas that recorded with picrotoxin occurred at 0.5 msec. Bicuculline prolonged the closed time, with a dominant closed time component at 52 msec. Elementary conductance was not altered by either agent. In conclusion, we found that the γ-aminobutyric acid type A channel antagonists picrotoxin and bicuculline were also blockers of embryonic nicotinic acetylcholine receptor channels in cultured rat muscle.

Skeletal muscles of invertebrates are innervated by excitatory and inhibitory fibers. Inhibition is mediated at pre- and postsynaptic sites by GABA, through Cl^- conductance (1–5). PTX and BIC block physiological and pharmacological inhibition at lobster and hermit crab neuromuscular junctions (6, 7). Similar effects of PTX have been observed in locust flexor tibialis muscle (8). In contrast, well developed vertebrate skeletal muscles are innervated only by excitatory cholinergic fibers. During the embryonic and early postnatal period, rat spinal cord motoneurons express GABA immunoreactivity (9). The transient GABA immunoreactivity in motoneurons during neuromuscular junction formation suggests that GABA may play an important role in its formation. These results have led us to study the effects of GABA and GABA-related substances on the electrical and chemical excitability of embryonic skeletal muscle maintained in culture in the absence of motoneurons. We have used whole-cell and single-channel recording techniques and report here that, although GABA had no detectable effects on either passive or active membrane properties or ACh-activated currents, both PTX and BIC, classical antagonists of GABA at $GABA_A$ receptor-coupled Cl^- channels, altered cholinergic responses via changes in channel kinetics rather than conductance. Some of these results have previously been reported in abstract form (10).

Materials and Methods

Cell culture. Skeletal muscle cells from rats of embryonic day 19 were dissociated into single-cell suspensions using a previously described trypsin digestion protocol (11). Briefly, muscle was dissected from the hindlimbs of embryos, minced, and digested with 0.05% trypsin in Ca^{2+}- and Mg^{2+}-free HEPES-buffered saline for 30 min at 37°. DNase I (0.01%) was included in the digestion medium to prevent myocyte aggregation. The dissociated cells were washed twice with DMEM, resuspended in 30 ml of DMEM, placed in a 100-mm plastic tissue culture dish, and incubated for 30 min at 37° to allow the preferential adhesion of fibroblasts. Myoblasts were then collected and resuspended in medium containing 80% DMEM, 10% fetal bovine serum, and 10% horse serum. Cells were plated at a density of 2.5 × 10^5 cells/ml in gelatin-coated, plastic, Petri dishes. After 3 days in culture, 10 μM cytosine arabinoside was added to inhibit outgrowth of any fibroblasts inadvertently left in the initial suspension. Two days thereafter, the medium was changed to one containing 90% DMEM and 10% horse serum.

ABBREVIATIONS: GABA, γ-aminobutyric acid; PTX, picrotoxin; BIC, bicuculline; ACh, acetylcholine; nAChR, nicotinic acetylcholine receptor; HEPES, 4-(2-hydroxyethyl)-1-piperazineethanesulfonic acid; DMEM, Dulbecco's modified Eagle medium; EGTA, ethylene glycol bis(β-aminoethyl ether)-*N*,*N*,*N*′,*N*′-tetraacetic acid.

Electrophysiological recordings and analysis. Experiments were performed on myotubes cultured between 3 and 14 days. Shortly before the experiment, the culture medium was replaced with extracellular recording solution containing 140 mM NaCl, 5.4 mM KCl, 0.8 mM $MgCl_2$, 1.8 mM $CaCl_2$, 10 mM HEPES, and 10 mM glucose, pH 7.4 (osmolarity, 310 mOsM). All recordings were carried out at room temperature (22–25°) on a Zeiss inverted microscope. The recording pipettes were pulled from 1.5-mm o.d., thin-walled, capillary tubes (WPI, Sarasota, FL) with a computer-controlled microelectrode puller (BB-CH-PC; Mecanex SA, Nyon, Switzerland). Electrical resistances of the pipettes ranged between 10 and 15 MΩ when the pipettes were filled with pipette solution. Pipettes used for cell-attached single-channel recordings were coated with Sylgard 184 (Dow Corning, Midland, MI) and filled with extracellular recording solution containing 4 μM ACh. PTX or BIC (both from Sigma) was added to the same solution when used. The pipette solution for whole-cell recordings contained 140 mM CsCl, 2 mM $MgCl_2$, 0.1 mM $CaCl_2$, 1.1 mM EGTA, 5 mM HEPES, 5 mM ATP, and 5 mM phosphocreatine, pH 7.2 (osmolarity, 290 mOsM). ACh was puffed to the myotube under low pressure, using a pipette positioned within 10 μm. Brief 1-sec pulses were applied every 40 sec to construct dose-response curves. The blocking agent was added either to the bath solution or to the ACh-containing pipette and applied together with ACh. Membrane currents were amplified with a List EPC-7 patch-clamp amplifier at a gain of 5 mV/pA, filtered with a Frequency Devices low-pass filter (type 902, eight-pole Bessel filter) at 5 kHz, and stored in digital form on video tapes using a VR-100 digital recorder (Instrutech Co., Mineola, NY) and a Panasonic videocassette recorder. Analyses were made off-line on a Dell system 310 computer. In cell-attached single-channel recordings, signals were further filtered at 2 kHz before being sampled and analyzed at 10 kHz with a TL-1 DMA interface and pCLAMP program (Axon Instruments, Foster City, CA). Single-channel nAChR currents have a square-wave appearance under control conditions; exposure to PTX invariably led to a flickering in the open state. Channel openings separated by any closed state, as defined by the "50% threshold" technique (12), were taken as single open events. Openings of ≤0.4 msec were discarded in the kinetic analysis. Data are expressed as mean ± standard error. Unpaired t tests were used to determine statistical significance; $p < 0.05$ was considered significant.

Results

GABA does not affect nAChR currents. Because motoneurons in the embryonic rat spinal cord exhibit GABA immunoreactivity both at the cell body level and in their axons issuing into the myotome, it was logical to test embryonic rat skeletal muscle cells for possible effects of GABA on their excitable membrane properties. In embryonic day 19 rat skeletal muscle cells cultured for 3–14 days, up to 1 mM GABA neither induced any current nor had any effect on either voltage-dependent currents or ACh-induced currents, when tested with whole-cell and single-channel recording techniques (data not shown). However, two $GABA_A$ receptor-coupled Cl^- channel blockers, PTX and BIC, affected ACh-induced channel activity in different ways.

PTX and BIC have different effects on ACh currents evoked in embryonic muscle. We studied the pharmacological effects of PTX and BIC on ACh-induced currents in whole-cell recordings. In these experiments, membrane potential was routinely held at −60 mV. Adding BIC cumulatively to the bath solution decreased the amplitude of ACh-induced current in a dose-dependent, reversible manner (Fig. 1A). BIC at 200 μM blocked ~90% nAChR current. In contrast, PTX had little if any effect; 600 μM PTX reduced the current by ~15% (Fig. 1B). We carried out experiments similar to that shown in Fig. 1 in a series of cells. Dose-response curves for BIC and PTX effects on ACh-induced current amplitudes are plotted in Fig. 2. PTX had no statistically significant effect on the current (−9% at 600 μM, $p > 0.05$), whereas BIC blocked the current in a dose-dependent manner. About 100 μM BIC blocked 50% of the current ($IC_{50} = 101.2 \pm 8.9$ μM, $n = 5$) and 250 μM BIC blocked the current by about 80%.

To further characterize the blocking effect of BIC, dose-response curves for ACh in the absence and presence of 200 μM BIC were compared (Fig. 3). The experimental values ($n = 4$ for all points) in both groups agreed well with the continuous theoretical curves calculated from the following equation:

$$I = I_{max} \frac{[ACh]^n}{[ACh]^n + K_d^n}$$

where I is the nAChR current, I_{max} is the maximum current, [ACh] is the concentration of ACh, K_d is the dissociation constant of ACh with nAChRs, and n is the Hill coefficient. In the absence of BIC, the best fit was obtained with $K_d = 25.4$ μM and $n = 1.88$, suggesting that a minimum of two molecules of ACh must bind to the nAChR before the channel opens. BIC at 200 μM reduced the maximum inducible nAChR current (normalized I_{max} decreased from 2182.4 to 116.9 relative units) without changing the K_d (22.9 μM), suggesting that BIC uncompetitively blocked ACh binding to nAChR.

PTX and BIC alter single-channel kinetics. The single-channel nAChR currents in cultured embryonic rat skeletal muscle recorded in the cell-attached configuration exhibited characteristic all-or-none transitions at +50 mV pipette potential (Fig. 4A). The mean open time was about 6 msec and the amplitude was about 4 pA, which was consistent with a channel conductance of about 36 pS, assuming that the resting membrane potential was −60 mV (see below). This indicates that the nAChR channels exhibit properties characteristic of the embryonic type for up to 2 weeks in culture. When 50 μM PTX was included in the pipette with ACh, the all-or-none transitions in current were often repeatedly and rapidly interrupted, so that bursts of brief openings appeared (Fig. 4B). The frequency of these bursts in the presence of PTX (48.3 sec^{-1}) was similar to that of relatively uninterrupted openings recorded in the absence of PTX (50.7 sec^{-1}). Additionally, the burst duration in the presence of PTX was comparable to the uninterrupted transitions characteristic of openings in the absence of PTX (compare Fig. 4, A and B). In contrast, 50 μM BIC decreased the frequency of channel openings (27.8 sec^{-1}) and the durations of individual openings (Fig. 4C). Neither PTX nor BIC changed the amplitude of the elementary current or channel conductance (see below). The mean amplitude of single-channel nAChR currents recorded at a pipette potential of +50 mV was 3.9 ± 0.1 pA ($n = 18$). The mean values in the presence of PTX and BIC were 3.8 ± 0.1 ($n = 14$, $p > 0.05$) and 3.8 ± 0.1 pA ($n = 11$, $p > 0.05$), respectively. Thus, both agents altered channel kinetics in quite different ways but did not affect elementary current amplitude.

The open time distributions were well fitted with one exponential component under control and experimental conditions. Examples of current-time histograms recorded in the absence and presence of ligands are illustrated in Fig. 5. A sample fitting of ACh-induced transitions recorded under control conditions was fitted with time constant (τ_o) of 5.8 msec (Fig. 5A). PTX at 50 μM markedly decreased τ_o to 1.7 msec (Fig. 5B). BIC at

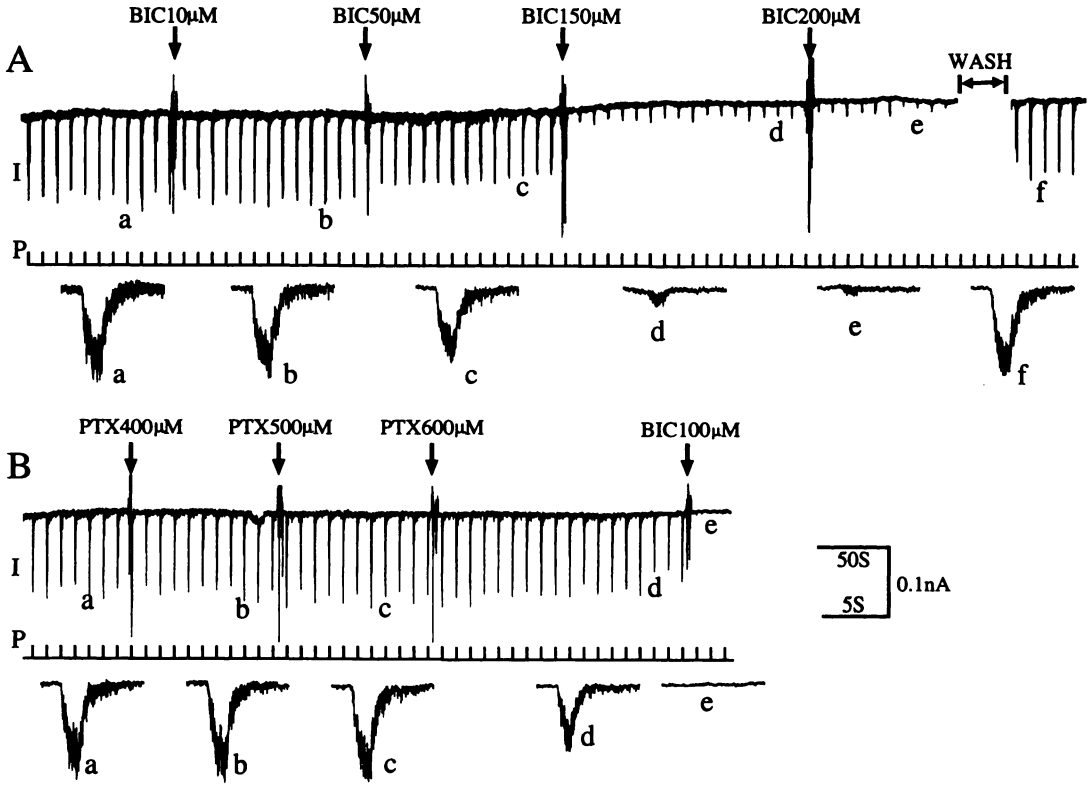

Fig. 1. Differential effects of PTX and BIC on whole-cell embryonic nAChR current. A, BIC added to the bath solution cumulatively blocked ACh-induced current gradually, and the current recovered completely after wash-out. B, PTX applied like BIC had little effect on the whole-cell nAChR current at a concentration of up to 600 μM. However, 100 μM BIC added later in addition to PTX blocked the current completely. *Upper continuous traces*, effects of PTX and BIC on nAChR current (*I*); *middle traces*, 2-sec applications of pressure to the puffing pipettes (*P*). *Arrows* and *numbers*, time and cumulative amount of PTX or BIC added. *Lower traces*, at higher time resolution, samples of nAChR current in each stage, as indicated by the same *letters*. Membrane potential was held at −60 mV. Calibrations apply to both panels. The *upper time scale* applies to *upper continuous recordings* and the *lower scale* applies to the *lower traces*.

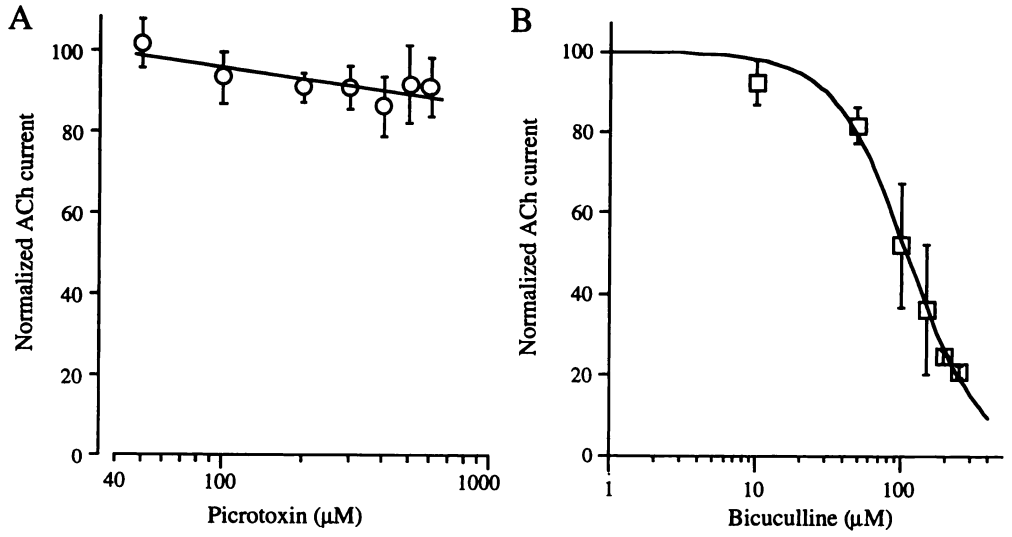

Fig. 2. Dose-effect curves for PTX and BIC effects on whole-cell embryonic nAChR current. A, PTX at up to 600 μM had little effect on whole-cell embryonic nAChR current. B, BIC blocked the current in a dose-dependent manner. The *curve* represents the least-squares fit to the data points for the relation $I = I_o \cdot K_i'^n/([B]^n + K_i'^n)$, where I_o is 100, K_i is the IC_{50}, and [B] is the BIC concentration. The IC_{50} for BIC is 109 μM; *n* is 1.72. ACh current was induced by puffing 4 μM ACh from a local pipette. PTX and BIC were added to the bath cumulatively. The current amplitudes in the presence of different concentrations of PTX or BIC were normalized to the current recorded before any antagonists were added. Holding potential was −60 mV. Each *point* was the mean of two to five tests.

50 μM also reduced τ_o but to a smaller degree (4.1 msec) (Fig. 5C). For 18 experiments under control conditions, the mean value of τ_o was 6.3 ± 0.5 msec (Fig. 5D). In the presence of 50 μM PTX, τ_o decreased to 1.7 ± 0.1 msec (−73%, $p < 0.01$), whereas 50 μM BIC decreased τ_o to 4.2 ± 0.6 msec (−33%, $p < 0.05$) (Fig. 5D).

Fig. 6 shows the closed time histograms obtained for each of the three experimental conditions. Two exponential functions adequately fitted all three histograms. Under control conditions (Fig. 6, *upper*), the dominant component (85% of the observed events) had a time constant of 17 msec, which represents the time between independent openings or bursts of openings. The short closed component of 0.5 msec represents the brief gaps due to repeated openings of a single channel. In the presence of 50 μM PTX (Fig. 6, *middle*), the brief closed component became dominant (86% of the events). This component corre-

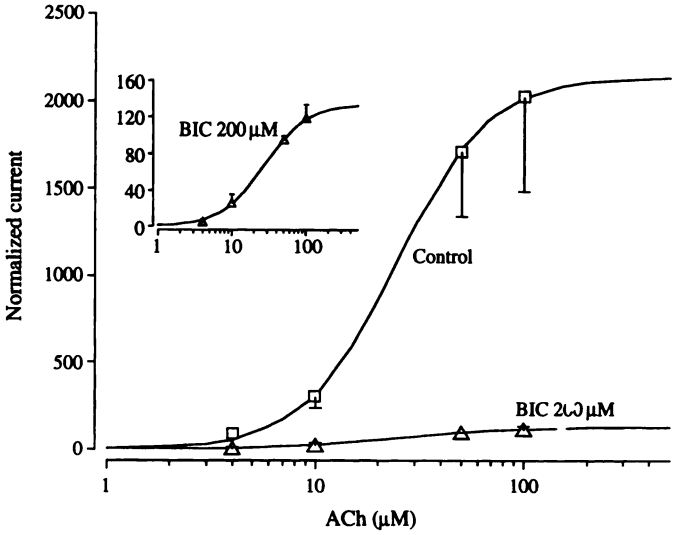

Fig. 3. Noncompetitive blocking effect of BIC on whole-cell embryonic nAChR current. The dose-response curves for ACh in the presence and absence of 200 μM BIC were normalized to the current evoked with 4 μM ACh. The calculated Hill coefficient for both groups (four experiments for each group) was 1.9. The K_d value and maximal response were 25.4 μM and 2182.4 relative units in the absence of BIC and 22.9 μM and 116.9 relative units in the presence of BIC, respectively. *Inset*, dose-response curve in the presence of 200 μM BIC plotted on a different scale. □, Normalized current in the absence of BIC; △, normalized current in the presence of BIC.

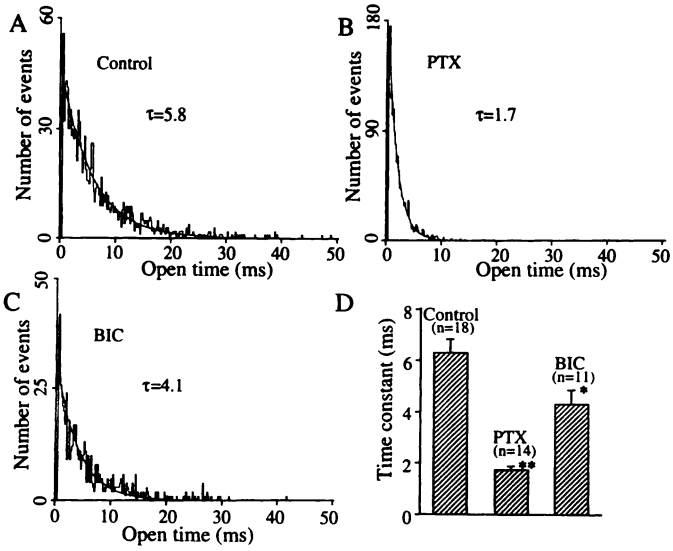

Fig. 5. Decreases by both PTX and BIC of the open time constant of embryonic single-channel nAChR current. Data were binned at 0.2 msec; the first two bins were not included in the analysis. A-C, One exponential component was adequate to fit control (A), PTX (B), and BIC (C) data. The time constants were 5.8, 1.7, and 4.1 msec in control, with 50 μM PTX, and with 50 μM BIC, respectively. D, A summary of a series of experiments is shown. The time constants were 6.3 ± 0.5, 1.7 ± 0.1, and 4.2 ± 0.6 msec (means ± standard errors) in control, with 50 μM PTX, and with 50 μM BIC, respectively. *Numbers in parentheses*, numbers of experiments for each group. *, $p < 0.05$; **, $p < 0.01$. Other details were as in Fig. 1.

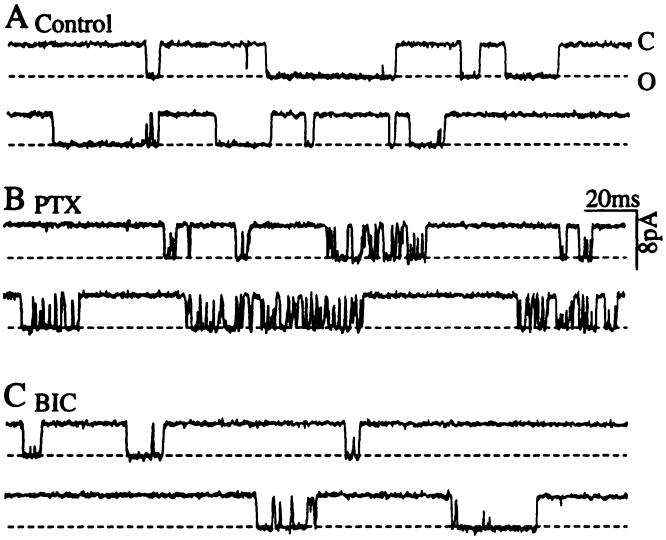

Fig. 4. Effects of PTX and BIC on the opening properties of embryonic nAChR single channels in cell-attached patch-clamp recordings. A, The single-channel openings in the control have a square-wave appearance and last from several milliseconds to tens of milliseconds. B, In the presence of 50 μM PTX, no long openings exist and brief openings tend to cluster together. Clusters of short openings are separated by closed states indistinguishable from those in the control recording. C, BIC at 50 μM reduces the number and duration of single-channel openings. The amplitudes of single-channel currents in control, PTX, and BIC recordings were 4.2, 4.0, and 4.2 pA, respectively. Pipette potential was held at +50 mV. Inward current is plotted downward. *Control*, single channels recorded with 4 μM ACh in the recording pipette; *PTX*, single channels recorded with 50 μM PTX and 4 μM ACh in the pipette; *BIC*, single channels recorded with 50 μM BIC and 4 μM ACh in the pipette. *O*, Open states; *C*, closed states.

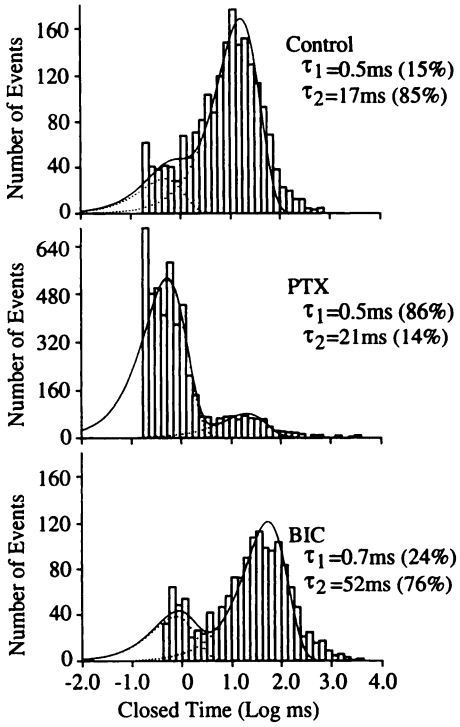

Fig. 6. Closed time histograms presented with a logarithmically binned time axis and fitted with a two-exponential function. The long component in each histogram represents the time between independent openings or bursts of channels, whereas the short component represents the brief gaps due to repeated openings of a single channel. *Numbers in parentheses*, fractional contribution of each component to the area under the curve.

sponds to the flickering gaps induced by PTX. The time between independent openings or bursts of openings was not changed by PTX (21 msec). In the presence of 50 μM BIC (Fig. 6, *lower*), the long component dominated, being three times longer (52 msec) than in control, indicating that the channel spends more time in a closed and/or blocked state. The short component was not modified by BIC.

Elementary conductance is not altered by either PTX or BIC. It was shown that, at a concentration of 50 μM, PTX and BIC had no effect on the amplitude (hence the point conductance) of nAChR current at a holding potential of +50 mV in cell-attached single-channel recordings (see above). In the studied range of pipette potentials of −125 to +80 mV in cell-attached single-channel recordings, the current-voltage curve was linear (Fig. 7). In the presence of 50 μM PTX or BIC, the current-voltage curves remained linear, and no significant changes in the reversal potential or slope conductance of the channel were observed (see Fig. 7). For 17 control experiments, the mean values for slope conductance and reversal potential were 35.4 ± 0.6 pS and −60.8 ± 3.3 mV, respectively. Because the major permeable ions for nAChR channels are Na^+ and K^+, the reversal potential of cell-attached single-channel current reflects the resting membrane potential. In 10 experiments in the presence of 50 μM PTX, slope conductance (34.3 ± 0.6 pS, $p > 0.05$) and reversal potential (−55.1 ± 4.3 mV, $p > 0.05$) were not significantly different from those of the controls. No significant changes were observed for either slope conductance (33.7 ± 0.7 pS, $p > 0.05$) or reversal potential (−63.3 ± 2.5 mV, $p > 0.05$) in the presence of 50 μM BIC in 12 experiments.

Discussion

The nAChRs expressed by skeletal muscle fibers are among the best characterized ion channels to date. nAChR-coupled channels recorded in embryonic rat skeletal muscle have lower conductance and longer open times before innervation by motoneurons than after the formation of functional neuromuscular junctions (13–16). These differences in channel properties correlate with changes in the molecular composition of nAChR subunit proteins that comprise the channel (17, 18). Extensive studies not only have greatly increased our understanding of both the structure and function of the muscle nAChR but also have made muscle nAChRs an excellent prototype for the family of neurotransmitter-gated membrane channels, which includes both muscle and neuronal nAChRs, GABA$_A$ receptors, glycine receptors, and possibly non-*N*-methyl-D-asparate excitatory amino acid receptors (19).

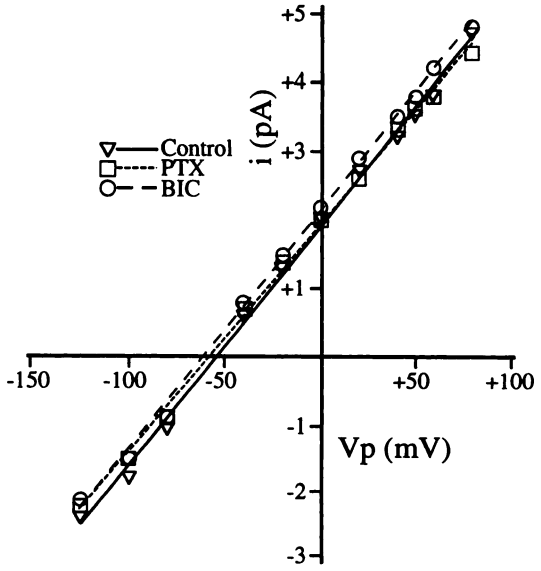

Fig. 7. Lack of significant change by PTX and BIC of the reversal potential or the slope conductance of embryonic single-channel nAChR current. The current-voltage curves were roughly linear in the range of pipette potentials of −125 to +80 mV. The reversal potential in the control was 53.6 mV and those with 50 μM PTX or BIC included in the recording pipettes were 57.7 and 60.3 mV, respectively. Conductances were 34.9, 33.1, and 34.8 pS in control and with PTX and BIC, respectively. *I*, Single-channel current; *Vp*, pipette potential.

There have been several reports describing the cross-reactivities of GABA$_A$ antagonists at ACh receptors. Benson (20) reported that BIC partially competitively blocked ACh-evoked cation channels in locust ganglion neurons. Experiments by Yarowsky and Carpenter (21) showed that PTX and BIC can block the Cl^- responses (but not Na^+ responses) to both ACh and GABA in *Aplysia* neurons. Zhang and Feltz (22) found that BIC can partially competitively block neuronal nAChR channels in cultured porcine intermediate pituitary lobe cells. On the other hand, studies by Schwartz and Mindlin (23) indicated that noncompetitive inhibitors of nAChR-gated cation channels inhibit GABA receptor-gated chloride ion channels in rat brain. Here we report that PTX and BIC, classical antagonists of GABA at GABA$_A$ receptor-coupled Cl^- channels, block embryonic-type nAChR channels in cultured rat myotubes. The mechanisms involved in these cross-reactions are still unclear. Molecular biology studies of neurotransmitter receptor structures have concluded that receptors with distinctly different functions can be related in their molecular structures. For example, nAChRs, which gate cation-selective channels in vertebrate skeletal muscle, are thought to belong to the same supergene family of molecular structures as do those receptors engaging GABA, which activate anion-selective channels in invertebrate muscle and vertebrate neurons and glial cells (24–26). Both nAChRs and GABA$_A$ receptors are assembled, in similar manners, from several transmembrane subunit proteins arranged around a corresponding central ion channel. Similar peptide segments in one or more subunits of nAChRs and GABA$_A$ receptors may form similar structures, serving as binding sites for their common agonists or antagonists. Embryonic- and adult-type nAChRs share common α, β and δ subunits but differ in their fourth component, which is γ for embryonic receptors and ε for adult receptors (17, 18). We did not observe any blocking effects of PTX or BIC on the adult-type nAChR (data not shown), suggesting that the binding sites of PTX and BIC are either on the γ subunit itself or on another site that is revealed when the receptor is configured with a γ subunit. The cross-reactivities between GABA$_A$ receptor antagonists and nAChR channels and between curariform drugs and GABA$_A$ receptor/Cl^- channels indicate that the ligands lack the pharmacological specificity that they are usually assumed to exhibit. Such cross-reactivities should be considered when these agents are used to identify and study either cholinergic or GABAergic transmissions at central or peripheral synapses.

Two classes of theories are used to explain ion channel-blocking mechanisms (27). Blocking agents either can bind within the channel pore itself, so that the flow of ions is impeded or stopped, or can bind to a site somewhere on the macromolecule and allosterically stabilize closed conforma-

tional states of the pore so that opening is less likely. Most of the time it is difficult to distinguish precisely which of the two mechanisms explains the blocking effect. For some ion channel blockers, the binding sites are exposed only when the channel is in the open state and the blocker must unbind before the channel can change to the closed state (28, 29). This is called the sequential blocking model and, in cases of nAChR channel blocking, can be represented with the following equation:

$$2A + R \rightleftarrows A_2R \rightleftarrows A_2R^* \rightleftarrows A_2R^*B$$

where A is the ACh molecule, R is the closed nAChR channel, R^* is the open nAChR channel, and B the channel blocker. In this case, if the residency time of the channel blocker at its binding site(s) is very short, so that binding, dissociation, and rebinding occur quickly, interrupted bursts of brief currents would be seen in single-channel recordings. This model also predicts that an increase in the number of openings per burst would completely compensate for the reduction in mean open time, so that little or no change in total charge flow per unit time would be detected. This phenomenon should be independent of the blocker concentration, because channels can recover from the blocked state only via the open state. Conceivably, the burst duration would be increased because it would be the sum of the durations of the open state plus the blocked state. In our experiments, PTX changed square wave-like long openings of embryonic-type single-channel nAChR currents in cultured rat skeletal muscle into clusters of very short current pulses, and up to 600 μM PTX had little effect on the whole-cell current. Therefore, the simple three-state sequential blocking model adequately describes the blocking action of PTX on the embryonic nAChR channel in cultured rat skeletal muscle. Although PTX is an effective blocker of the embryonic rat skeletal muscle nAChR channel, the fact that it had little impact on the whole-cell current suggests that it may not be a potent inhibitor of neuromuscular transmission mediated by embryonic-type nAChRs.

It has been questioned whether BIC is a specific $GABA_A$ receptor antagonist (30, 31). BIC has a very weak effect or no effect on neurally evoked GABA-mediated neuromuscular inhibition or on the action of GABA applied to crustacean muscle fibers (6, 32–34). Zhang and Feltz (22) reported that, in pituitary intermediate lobe cells of the pig, BIC partially competitively blocked neuronal nAChR channels, suggesting that BIC could compete with ACh for binding sites. The blocking effect of BIC on embryonic rat skeletal muscle nAChR channels was dose dependent and noncompetitive. The precise blocking mechanism of BIC is not clear. More experiments should be carried out to clarify whether PTX and BIC can increase the rate of desensitization of the embryonic nAChR channels, like some other blockers (35–37). PTX and BIC did not change either the conductance or the reversal potential of embryonic nAChRs, suggesting that these compounds do not affect the ion selectivity of the channel. After 10 days in culture, adult-type events (conductance of ~60 pS and open time of ~1 msec) appeared but comprised <1% of single-channel events. There appeared to be no detectable differences in the properties of adult-type single channels recorded in controls or with PTX or BIC, although systematic analysis was not made because of the limited number of events.

Acknowledgments

We thank Drs. Jean Vautrin, Ruggero Serafini, and Yong-Xin Li for their critical reviews of the manuscript and helpful suggestions and Devera G. Schoenberg for editorial assistance. Q.Y.L. thanks Dr. Anne Schaffner for advice in preparing cell cultures.

References

1. Boistel, J., and P. Fatt. Membrane permeability change during inhibitory transmitter action in crustacean muscle. *J. Physiol. (Lond.)* **144**:176–191 (1958).
2. Dudel, J., and S. W. Kuffler. Presynaptic inhibition at the crayfish neuromuscular junction. *J. Physiol. (Lond.)* **155**:543–562 (1961).
3. Takeuchi, A., and N. Takeuchi. Anion permeability of the inhibitory postsynaptic membrane of the crayfish neuromuscular junction. *J. Physiol. (Lond.)* **191**:575–590 (1967).
4. Gerschenfeld, H. M. Chemical transmission in invertebrate central nervous systems and neuromuscular junctions. *Physiol. Rev.* **53**:1–119 (1973).
5. Atwood, H. L. Organization and synaptic physiology of crustacean neuromuscular systems. *Prog. Neurobiol.* **7**:291–391 (1976).
6. Shank, R. P., S. F. Pong, A. R. Freeman, and L. T. Graham, Jr. Bicuculline and picrotoxin as antagonists of γ-aminobutyrate and neuromuscular inhibition in the lobster. *Brain Res.* **72**:71–78 (1974).
7. Earl, J., and W. A. Large. Electrophysiological investigation of GABA-mediated inhibition at the hermit crab neuromuscular junction. *J. Physiol. (Lond.)* **236**:113–127 (1974).
8. Werman, R., and N. Brookes. Interaction of γ-aminobutyric acid with postsynaptic inhibitory receptor of insect muscle. *Fed. Proc.* **28**:831 (1969).
9. Ma, W., T. Behar, and J. L. Barker. Transient expression of GABA immunoreactivity in the developing rat spinal cord. *J. Comp. Neurol.* **325**:271–290 (1992).
10. Liu, Q. Y., V. Smallwood, and J. L. Barker. $GABA_A$ antagonists picrotoxin and bicuculline alter nicotinic acetylcholine channel kinetics in cultured embryonic rat myotubes. *Soc. Neurosci. Abstr.* **18**:189.13 (1992).
11. Schaffner, A. E., P. A. St. John, and J. L. Barker. Fluorescence-activated cell sorting of embryonic mouse and rat motoneurons and their long-term survival *in vitro*. *J. Neurosci.* **7**:3088–3104 (1987).
12. Coquhoun, D., and F. J. Sigworth. Fitting and statistical analysis of single-channel records, in *Single-Channel Recordings* (B. Sakmann and E. Neher, eds.). Plenum, New York, 191–263 (1983).
13. Siegelbaum, S. A., A. Trautmann, and J. Koenig. Single acetylcholine-activated channel currents in developing muscle cells. *Dev. Biol.* **104**:366–379 (1984).
14. Schuetze, S. M., and L. W. Role. Developmental regulation of nicotinic acetylcholine receptors. *Annu. Rev. Neurosci.* **10**:403–457 (1987).
15. Kidokoro, Y. Developmental changes in acetylcholine receptor channel properties of vertebrate skeletal muscle, in *Ion Channels* (T. Narahashi, ed.), Vol. 1. Plenum, New York, 163–182 (1988).
16. Jaramillo, F., and S. M. Schuetze. Kinetic differences between embryonic- and adult-type acetylcholine receptors in rat myotubes. *J. Physiol. (Lond.)* **396**:267–296 (1988).
17. Witzemann, V., B. Barg, M. Criado, E. Stein, and B. Sakmann. Developmental regulation of five subunit specific mRNAs encoding acetylcholine receptor subtypes in rat muscle. *FEBS Lett.* **242**:419–424 (1989).
18. Witzemann, V., E. Stein, B. Barg, T. Konno, M. Koenen, W. Kues, M. Criado, M. Hofmann, and B. Sakmann. Primary structure and functional expression of the α-, β-, γ-, δ- and ε-subunits of the acetylcholine receptor from rat muscle. *Eur. J. Biochem.* **194**:437–448 (1990).
19. Stroud, R. M., M. P. McCarthy, and M. Shuster. Nicotinic acetylcholine receptor superfamily of ligand-gated ion channels. *Biochemistry* **29**:11009–11023 (1990).
20. Benson, J. A. Bicuculline blocks the response to acetylcholine and nicotine but not to muscarine or GABA in isolated insect neuronal somata. *Brain Res.* **458**:65–71 (1988).
21. Yarowsky, P. J., and D. O. Carpenter. A comparison of similar ionic responses to γ-aminobutyric acid and acetylcholine. *J. Neurophysiol.* **41**:531–541 (1978).
22. Zhang, Z. W., and P. Feltz. Bicuculline blocks nicotinic acetylcholine response in isolated intermediate lobe cells of the pig. *Br. J. Pharmacol.* **102**:19–22 (1991).
23. Schwartz, R. D., and M. C. Mindlin. Inhibition of the GABA receptor-gated chloride ion channel in brain by noncompetitive inhibitors of the nicotinic receptor-gated cation channel. *J. Pharmacol. Exp. Ther.* **244**:963–970 (1987).
24. Schofield, P. R., M. G. Darlison, N. Fujita, D. R. Burt, F. A. Stephenson, H. Rodriguez, L. M. Rhee, J. Ramachandran, V. Reale, T. A. Glencorse, P. H. Seeburg, and E. A. Barnard. Sequence and functional expression of the $GABA_A$ receptor shows a ligand-gated receptor super-family. *Nature (Lond.)* **328**:221–227 (1987).
25. Lindstrom, J., R. Schoepfer, and P. Whiting. Molecular studies of the neuronal nicotinic acetylcholine receptor family. *Mol. Neurobiol.* **1**:218–337 (1987).
26. Barnard, E. A., M. G. Darlison, and P. Seeburg. Molecular biology of the $GABA_A$ receptor: the receptor/channel superfamily. *Trends Neurosci.* **10**:502–509 (1987).

27. Hille, B. *Ionic Channels of Excitable Membranes*, Ed. 2. Sinauer Associates, Sunderland, MA (1992).
28. Adams, P. R. Drug blockade of open end-plate channels. *J. Physiol. (Lond.)* **260**:531–552 (1976).
29. Neher, E., and J. H. Steinbach. Local anesthetics transiently block currents through single acetylcholine-receptor channels. *J. Physiol. (Lond.)* **277**:153–176 (1978).
30. Godfraind, J. M., K. Krnjevic, and R. Pumain. Doubtful value of bicuculline as a specific antagonist of GABA. *Nature (Lond.)* **228**:675–676 (1970).
31. Straughan, D. W., M. J. Neal, M. A. Simmonds, G. G. S. Collins, and R. G. Hill. Evaluation of bicuculline as a GABA antagonist. *Nature (Lond.)* **233**:352–354 (1971).
32. Earl, J., and W. A. Large. The effects of bicuculline, picrotoxin and strychnine on neuromuscular inhibition in hermit crabs (*Eupagurus bernhardus*). *J. Physiol. (Lond.)* **224**:45P–46P (1972).
33. Swagel, M. W., K. Ikeda, and E. Roberts. Effects of GABA and bicuculline on conductance of crayfish abdominal stretch receptor. *Nature New Biol.* **244**:180–181 (1973).
34. Takeuchi, A., and K. Onodera. Effect of bicuculline on the GABA receptor of the crayfish neuromuscular junction. *Nature New Biol.* **236**:55–56 (1972).
35. Burgermeister, W., W. A. Catterall, and B. Witkop. Histrionicotoxin enhances agonist-induced desensitization of acetylcholine receptor. *Proc. Natl. Acad. Sci. USA* **74**:5754–5758 (1977).
36. Carp, J. S., R. S. Aronstam, B. Witkop, and E. X. Albuquerque. Electrophysiological and biochemical studies on enhancement of desensitization by phenothiazine neuroleptics. *Proc. Natl. Acad. Sci. USA* **80**:310–314 (1983).
37. Kaldany, R. R., and A. Karlin. Reaction of quinacrine mustard with the acetylcholine receptor from *Torpedo californica*. *J. Biol. Chem.* **258**:6232–6242 (1983).

Send reprint requests to: Qi-Ying Liu, Laboratory of Neurophysiology, NINDS, National Institutes of Health, Building 36, Room 2C02, Bethesda, MD 20892.